

Proceedings Article

Single-sided magnetic particle imaging devices using ferrite core to improve penetration depth

Qibin Wang^{a,b,c}. Zhonghao Zhang^{a,b,c}. Chenxiao Xu^{a,b,c}. Pengyue Guo^{a,b,c}. Yidong Liao^{a,b,c}.
Ning He^{a,b,c}. Yunpeng Gao^{a,b,c}. Lei Li^{a,b,c}. Shouping Zhu^{a,b,c,*}

^aSchool of Life Science and Technology, Xidian University & Engineering Research Center of Molecular and Neuro Imaging, Ministry of Education, Xi'an, Shaanxi 710126, China

^bXi'an Key Laboratory of Intelligent Sensing and Regulation of trans-Scale Life Information & International Joint Research Center for Advanced Medical Imaging and Intelligent Diagnosis and Treatment, School of Life Science and Technology, Xidian University, Xi'an, Shaanxi 710126, China

^cInnovation Center for Advanced Medical Imaging and Intelligent Medicine, Guangzhou Institute of Technology, Xidian University, Guangzhou, Guangdong 51055, China

*Corresponding author, email: spzhu@xidian.edu.cn

© 2023 Wang *et al.*; licensee Infinite Science Publishing GmbH

This is an Open Access article distributed under the terms of the Creative Commons Attribution License (<http://creativecommons.org/licenses/by/4.0>), which permits unrestricted use, distribution, and reproduction in any medium, provided the original work is properly cited.

Abstract

Single-sided MPI devices provide images from regions outside of an enclosed scanner but are limited by the penetration depth of these devices. To solve this problem, we propose adding a ferrite core to the coil to enhance the magnetic flux density. To improve the performance of the receiver coil, we use a spiral receiving coil to enhance the system's sensitivity. In addition, this work uses the permanent magnet array with adjustable magnetic block angle to generate a variable magnetic gradient strength and move the FFP position. The single-sided MPI system we designed in this work is a portable device, expected to achieve more accurate detection of tumor location and minimal removal of normal cells during breast-conserving surgery. Through simulation and analysis of measurement results, the feasibility of the device is verified.

1. Introduction

Magnetic particle imaging (MPI) is an emerging imaging modality that has yet to be applied in the clinic but has great potential [1]. Single-sided MPI devices place the components, such as coils, on one side of the system, allowing the size of the object to be measured unlimited, making it one of the systems with the most potential for clinical [2]. Currently, single-sided MPI devices include using field-free lines (FFL) [1] and field-free points (FFP) to find breast cancer sentinel lymph nodes [3]. In addition, single-sided MPI devices for breast-conserving

surgery with minimal removal of normal cells have been proposed [4][5]. However, the low magnetic field efficiency of single-sided MPI devices limits the penetration depth, which is an important issue in limiting single-sided MPI devices.

To solve these problems, we propose an improved single-sided MPI structure. To enhance the penetration depth of the system, a ferrite core is used for magnetic flux density enhancement, and a segmented excitation coil and a spiral receiving coil are used to improve the system's sensitivity. In combination with the permanent magnet array configuration, variable magnetic gradient

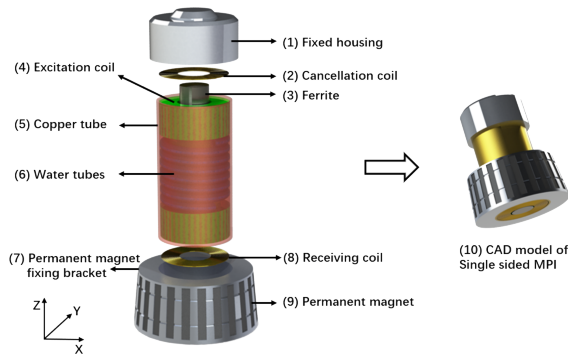


Figure 1: Schematic Diagram of Equipment Hardware Composition: (1) Fixed housing, (2) Cancellation coil, (3) Ferrite core, (4) Excitation coil, (5) Copper tube, (6) Water tubes, (7) Permanent magnet fixing bracket, (8) Receiving coil, (9) Permanent magnet, (10) CAD model of Single-sided MPI.

Table 1: Parameters of ferrite materials

Material	μ_i	μ_{max}	ρ	f
Mn-Zn ferrites (PC40)	2300 $H m^{-1}$	5000 $H m^{-1}$	65~85 $\mu\Omega \cdot cm$	1~5000 kHz

strength and moving FFP position are achieved on one side of the device by changing the angle of the permanent magnet block.

II. Material and methods

II.I. Single-sided MPI model and material

The device consists of 9 parts, as shown in Figure 1. To flexibly hold and drive the single-sided MPI system by a mechanical device, a fixing housing (1) is designed. Ferrite is a ceramic material with iron oxide as its main component. Its main characteristics are narrow and long hysteresis lines, high permeability, high resistivity, low loss, etc. As the magnetic field strength on one side of the single-sided MPI device decreases rapidly, adding a ferrite core (3) to the coil can enhance the magnetic flux density. To minimize the harmonic signal from the ferrite core, the ferrite core is placed in the center of the coil. This work uses Mn-Zn ferrite core, PC40 material, and its parameters are shown in Table 1. Initial permeability, maximal permeability, resistivity and frequency are denoted by μ_i , μ_{max} , ρ , and f , respectively.

The magnetic field used to excite the oscillating magnetic particles is generated by the excitation coil (4), which has a segmented structure using Leeds wire winding. In this work, we designed a spiral receiving coil (8) with higher sensitivity for the single-sided MPI devices. In contrast, there is a spiral canceling coil (2) of the same

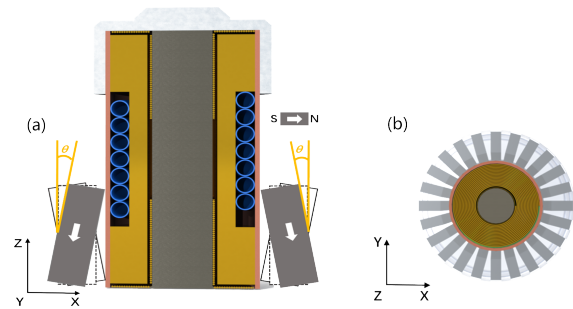


Figure 2: (a) Sectional view of single-sided MPI equipment. (b) Bottom view of equipment.

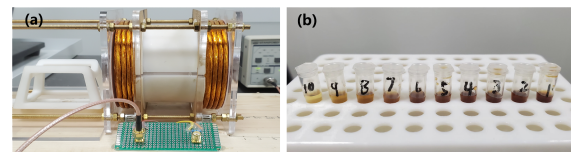


Figure 3: (a) Picture of the prototype (b) Equally diluted Perimag solution.

size but would reverse on the device's upper part.

The external electromagnetic environment and coil temperature are important for the stable operation of the system, so we added a copper tube (5) in the outer layer to shield the outside world from complex electromagnetic waves, a water tube (6) was designed in the middle to stabilize the coil temperature.

Permanent magnet arrays are flexible to use and have a high utilization of permanent magnets. In this work, by varying the angle of the permanent magnets (9) around the coil, a magnetic gradient field can be generated on one side of the device. In addition, the permanent magnet block can be rotated by different angles θ , thus moving the FFP position and changing the magnetic gradient strength. The direction of magnetization of the permanent magnet is shown by the white arrow in Figure 2(a).

II.II. Experiments

Simulation: In order to verify the magnetic gradient fields formed by the permanent magnet array, use the COMSOL 6.0 software to build a three-dimensional model. We simulated the magnetic gradient fields formed by the permanent magnet array in the XY plane, ZY planes, X-axis, and Z-axis. Changing the rotation angle of the permanent magnet block can move the FFP position and adjust the magnetic gradient strength.

We also used COMSOL software to simulate the size of the receiving coil, the number of turns and other parameters. By using the optimal structural parameters of the coil for the prototype, we can obtain better system performance.

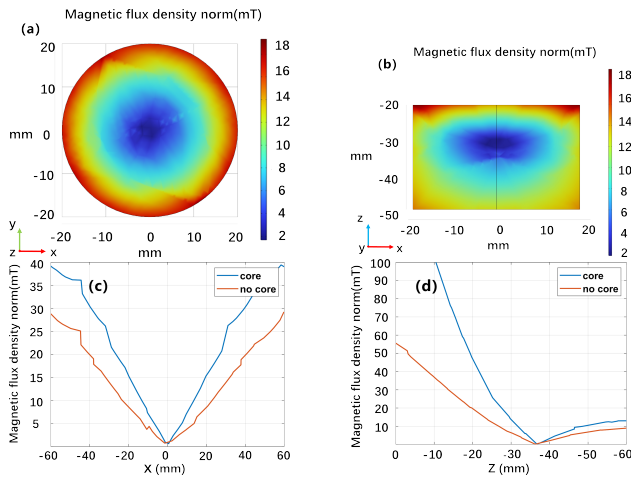


Figure 4: (a) XY-plane and (b) ZY-plane show the magnetic flux density norm with ferrite core when the FFP is at 34.3mm. (c) X-axis and (d) Z-axis show the comparison of magnetic flux density norm with and without ferrite core when the FFP is at about 34mm.

Measurements: In this work, to verify the performance of the system, a prototype was built based on the results of simulation experiments, as shown in Figure 3(a). Currently, the prototype tests the coil's penetration depth performance and the system's linearity after adding a ferrite core. However, the measurement experiment in this work was carried out without the permanent magnet array. By diluting the Perimag stock solution containing different Fe into 10 sets of samples of the same volume (100uL) of the resolution, as shown in Figure 3(b).

The device uses a signal generator (Keysight 33500B series) to generate a 25 kHz excitation signal, passed through a power amplifier (AE Techron 7224, 1kW). A 12A current is then applied to the excitation coil for oscillating the magnetic nanoparticles. The receiving coil picks up the oscillated particle's third harmonic (75 kHz). Before being acquired, the signal of magnetic nanoparticles passed through a high-pass filter (ZFHP-0R055-S+), a low-noise amplifier (SR560 with 1000x amplification), a lock-in amplifier (HF2LI, focusing only on the 75kHz), and finally was connected to an acquisition card for signal data acquisition (sampling rate of 625kHz/s).

III. Results

III.I. Simulation result

Figure 4 (a) and (b) show the simulation results of the magnetic flux density norm with ferrite core when the FFP is 34.3 mm. At this time, the permanent magnet block is rotated by 0 degrees. In order to show the effect on magnetic gradient strength with ferrite core, Figure 4 (c) X-axis and (d) Z-axis offer the comparison of magnetic flux density norm with and without ferrite core when

Table 2: Magnetic block rotation angle simulation results when with and without the ferrite core

Rotation angle θ	Location of FFP / (mm)	Gradient in Z-axis ($T m^{-1}$)	Gradient in X/Y-axis ($T m^{-1}$)
	core/no core	core/no core	core/no core
-10°	28.0/11.6	5.58/4.24	1.45/1.88
-5°	30.8/16.2	4.23/3.22	1.05/1.50
0°	34.3/22.5	3.14/2.15	0.75/0.96
5°	39.0/27.7	2.12/1.80	0.52/0.66
10°	47.5/34.5	1.17/1.36	0.34/0.50

the FFP is at about 34 mm. At this time, the permanent magnet block with ferrite core rotates 0 degrees, and the permanent magnet block without ferrite core rotates 10 degrees.

The magnetic gradient strength in the XY plane is relatively uniform. In contrast, the magnetic gradient strength in the ZX or ZY plane is unevenly distributed, with a large magnetic gradient strength on the side close to the device. By changing the rotation angle θ of the permanent magnet block, the position of the FFP can be moved, and the magnetic gradient strength can be changed. After adding a ferrite core, the FFP location shifts away from the device, and the magnetic gradient strength increases at the same FFP position. The simulation results are shown in Table 2, and the location of FFP is measured from the bottom of the device.

III.II. Linear system response measurement results

The procedure of the experiment. First, 100uL of distilled water was used for testing, 20ug of Fe was added sequentially to collect particle signals, and four repetitions of each experimental group were performed. The results of the four repeated tests were finally normalized, and four repeated experiments were named S1, S2, S3, and S4. The results are shown in Figure 5.

To minimize the harmonic signal from the ferrite core, the ferrite core is placed in the center of the coil so that the harmonic signal effect caused by the ferrite core can be minimized by using the cancellation coil. However, the harmonic signal effect caused by ferrite cannot be eliminated only by passive cancellation. By way of testing, the baseline change caused by ferrite is fixed so that it can be processed later.

The measurement results showed that the system still showed a linear increment with increasing mass of Fe after the device added the ferrite core. Still, the error of repeated experiments started to grow with more than 140ug Fe in the solution.

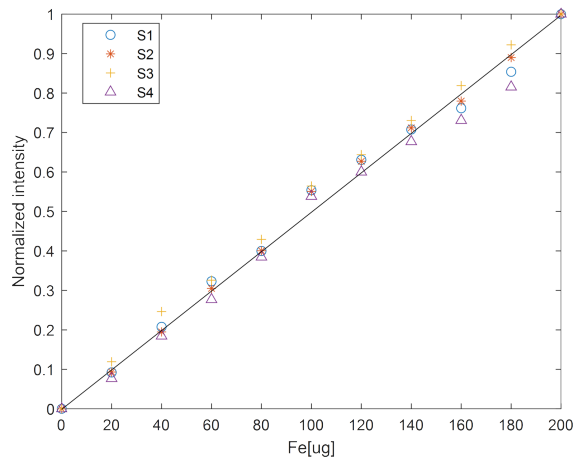


Figure 5: Perimag plot of the intensities at each dilution step.

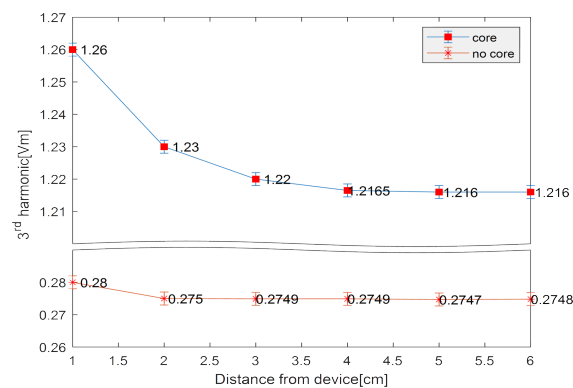


Figure 6: Perimag plot of the intensities at a different distance from the device (cm).

III.III. System penetration depth measurement results

Without using permanent magnets, the experiment was carried out at different distances using 100uL (80ug Fe) Perimag solution samples. The blue curve represents the magnetic nanoparticle signal collected after the ferrite core's addition. The orange curve represents the magnetic nanoparticle signal assembled without adding the ferrite core. In order to show the comparison results more visually on one graph, a segment of the vertical coordinate values is hidden in the middle of Figure 6, which does not change the index value of the vertical coordinate.

As can be seen from Figure 6, the device can collect the sample signal even at 3cm after adding the ferrite core, while the device without the ferrite core can only detect the sample's signal at 1cm.

This shows that adding a ferrite core to the device not only improves the penetration depth, but also amplifies the particle signal.

IV. Conclusions

In this work, we designed a portable single-sided MPI device. The maximum penetration depth of the single-sided MPI device can be increased by adding a ferrite core to the coil. The system's sensitivity is improved by altering the coil structure, including using spiral receiving coils and segmented excitation coils. The magnetic gradient field generated by permanent magnet array has been verified by simulation, and the measurement will be done in future work. The device is expected to be applied to detect tumor cells and maximize the removal of cancer cells during breast-conserving surgery.

Acknowledgments

This work was supported by the National Natural Science Foundation of China under Grant Nos. 62027901, 62071362, 82272050, 61901342, the Natural Science Basic Research Program of Shaanxi Province under Grant Nos. 2021JZ-29, 2021SF-131, 2021SF-169, and the Fundamental Research Funds for the Central Universities under Grant No. JB211205.

Author's statement

Conflict of interest: Authors state no conflict of interest.

References

- [1] Tonyushkin A. Single-sided field-free line generator magnet for multi-dimensional magnetic particle imaging[J]. IEEE Transactions on Magnetics, 2017, pp. 1-6.
- [2] Gräfe K, von Gladiss A, Bringout G, et al. 2D images recorded with a single-sided magnetic particle imaging scanner[J]. IEEE transactions on medical imaging, 2015, pp. 1056-1065.
- [3] Soares Y B, Lüdtkke-Buzug K, von Gladiss A, et al. Further system characterization of the Single-Sided MPI Scanner with two-and three-dimensional measurements[J]. International Journal on Magnetic Particle Imaging, 2021, 7(2).
- [4] Choi S H, Le T A, Son B, et al. A portable single-sided magnetic particle imaging concept using amplitude modulation for breast conserving surgery [J]. International Journal on Magnetic Particle Imaging, 2022, 8.
- [5] Mason E E, Mattingly E, Herb K, et al. Concept for using magnetic particle imaging for intraoperative margin analysis in breast-conserving surgery[J]. Scientific Reports, 2021, pp. 1-16.